JOURNAL OF CATALYSIS 145, 267–275 (1994)

On the Mechanism of *n*-Butane Oxidation to Maleic Anhydride on VPO Catalysts

II. Study of the Evolution of the VPO Catalysts under *n*-Butane, Butadiene, and Furan Oxidation Conditions

Y. Zhang-Lin,* M. Forissier,† J. C. Védrine,* and J. C. Volta*

*Institut de Recherches sur la Catalyse, CNRS, 2 Avenue A. Einstein, 69626, Villeurbanne, Cédex, France; and †Génie catalytique des Réacteurs de Raffinage, CNRS-ELF, CRES, BP 22, 69360, St. Symphorien d'Ozon, France

Received May 5, 1993; revised July 12, 1993

The evolution of the $VOPO_4$ phases and of $(VO)_2P_2O_7$ and the activated VPO catalyst has been studied by XRD, ^{31}P MAS–NMR, laser Raman spectroscopy, and electron spin resonance after the oxidation of butane, butadiene, and furan. With the exception of δ $VOPO_4$, which partly changes to α_{II} $VOPO_4$, almost no evolution of the bulk structure has been observed. It is concluded that the mechanism of butane oxidation on the VPO catalyst implies principally the participation of a limited number of superficial layers of the structure. Catalytic properties depend on the redox properties of a limited number of V^{5+} ensembles on the $(VO)_2P_2O_7$ matrix. A proposal for the mechanism of *n*-butane oxidation which implies an alkoxide route is presented. © 1994 Academic Press, Inc.

INTRODUCTION

In a previous publication (1), we studied the oxidation of *n*-butane, butadiene, furan, and maleic anhydride (MA) on different phases of the VPO phase diagram, namely, α_{II}, β, γ, and δ $VOPO_4$ phases (V^{5+}), on $(VO)_2P_2O_7(V^{4+})$, and on the VPO catalyst (mainly $(VO)_2P_2O_7(V^{4+})$) obtained from the $VOHPO_4 \cdot 0.5H_2O$ precursor by activation in the butane/air atmosphere. A direct route to maleic anhydride which implies alkoxides intermediates without desorption in the gas phase of the intermediates butene, butadiene, and furan was proposed for the oxidation of butane on these different catalysts as an alternative to the olefinic route generally proposed for this reaction (2). The activated VPO catalyst was observed to be more selective to MA than was $(VO)_2P_2O_7$ for butane oxidation, while α_{II} $VOPO_4$ was observed to be rather dehydrogenating to butadiene, β $VOPO_4$ to be responsible for total oxidation, and γ and δ $VOPO_4$ to be fairly selective to MA. The eventual evolution of the physicochemistry of the corresponding materials in catalytic conditions was not taken into consideration in this previous work. Such an evolution may be considered as probable insofar as the oxidoreducing state of oxides, used as catalysts in oxidation, is dependent on temperature, on the composition of the catalytic atmosphere, and particularly on the more or less reducing power of the hydrocarbon (HC) used as reactant. For the same O_2/HC ratio, it is obvious that butadiene does not play the same role as furan or butane which are known to be chemically more inert. We have previously reported the transformation of δ $VOPO_4$ under butane/air (2.4%) into α_{II} $VOPO_4$, as evidenced by laser Raman spectroscopy in an *in situ* cell (3).

In the present work, the modifications of the different VPO catalysts under the oxidation of butane, butadiene, and furan are studied by XRD, laser Raman spectroscopy, ESR, and ^{31}P MAS–NMR. A model of the active site for *n*-butane oxidation to maleic anhydride on VPO catalysts is then proposed.

EXPERIMENTAL

Preparation and characterization of the different VPO catalysts including reference phases has been previously described in Ref. (1).

Preparation of Reference Phases

Pure VPO phases were prepared from three precursors: $VOPO_4 \cdot 2H_2O$, $NH_4(VO_2)_2PO_4$, and $VO(HPO_4) \cdot 0.5H_2O$. $VOPO_4 \cdot 2H_2O$ was prepared as described in Refs. (4–6) by heating V_2O_5 with 85% H_3PO_4 ($P/V = 7$) under reflux for 16 h. $NH_4(VO_2)_2PO_4$ was obtained according to Refs. (6, 7) by adding 85% H_3PO_4 to a solution of NH_4VO_3 10^{-2} M heated at 60°C ($P/V = 1$). $VO(HPO_4) \cdot 0.5H_2O$ was prepared according to Ref. (8) by refluxing a suspension of V_2O_5 in isobutanol in the presence of 85% H_3PO_4 ($P/V = 1.1$). After preparation, all products were collected and stored under dry argon to avoid rehydration.

0021-9517/94 $5.00

$(VO)_2P_2O_7$ was obtained by dehydration of $VO(HPO_4) \cdot 0.5H_2O$ under nitrogen at 700°C for 6 h (heating rate 75°C · h^{-1}). α_{II} $VOPO_4$ was prepared from $VOPO_4 \cdot 2H_2O$ by dehydration in dry air at 750°C for 17 h (heating rate 240°C · h^{-1}). β $VOPO_4$ was obtained by decomposition of $NH_4(VO_2)_2PO_4$ in dry air at 600°C for 10 h (heating rate 75°C · h^{-1}). γ $VOPO_4$ was prepared by oxydehydration of $VO(HPO_4) \cdot 0.5H_2O$ at 680°C for 4 h under dry oxygen (heating rate 110°C · h^{-1}). δ $VOPO_4$ was obtained from $VO(HPO_4) \cdot 0.5H_2O$ by oxydehydration in dry oxygen at 450°C during 168 h (heating rate 60°C · h^{-1}). These conditions led to well crystallized materials. The conditions of preparation from the precursors were chosen following the work by Bordes and Courtine (6).

Preparation of the Activated VPO Catalyst

The activated VPO catalyst was prepared from $VO(HPO_4) \cdot 0.5H_2O$ as described in Ref. (9). Activation was performed at 440°C under the following catalytic conditions: $C_4H_{10}/O_2/He = 1.2/16.4/82.4$; VSHV = 1200 h^{-1} for 48 h. These conditions corresponded to an "equilibrated catalyst," i.e., at stationary state, since catalytic and physicochemical characteristics were observed not to change with further time on stream (9).

Catalyst Characterization

Before and after the catalytic tests described, all samples were characterized by XRD, laser Raman spectroscopy (LRS), ESR, and ^{31}P MAS–NMR. X-ray diffraction patterns of the samples were recorded with a Siemens diffractometer using Cu K_α radiation. Raman spectra were recorded with a Dilor Omars 89 spectrophotometer equipped with an intensified photodiode array detector. The emission at 514.5 nm from an Ar^+ ion laser (Spectra Physics, Model 164) was used for excitation. The power of the incident beam on the sample was 36 mW. The time of acquisition was adjusted according to the intensity of the Raman scattering; 30 to 100 spectra were accumulated in order to improve signal to noise ratio. The wavenumber values obtained from the spectra were accurate to within about 2 cm^{-1}. The scattered light was collected in the back-scattering geometry.

The ESR measurements were performed on a Varian E9 spectrometer operating in the X-band mode. DPPH was used as a standard for g-value determinations using a dual cavity. Spectra were recorded at liquid and room temperatures.

The ^{31}P spectra were recorded with a Bruker MSL-300 spectrometer operating at 121.4 MHz. They were obtained under MAS conditions by use of a double-bearing probehead. A single pulse sequence was used in all cases and the delays were chosen to allow the obtention of quantitative spectra (typically the pulse width was 2 μs (10°) and the delay was 10 to 100 s). The number of scans was 10 to 100. The spectra were referred to external H_3PO_4 (85%). XRD, LRS, and ^{31}P MAS–NMR spectra of the pure reference phases have been published elsewhere (3).

RESULTS

Table 1 summarizes the evolution of the $VOPO_4$ phases due to the catalytic reaction as evidenced by XRD, ^{31}P

TABLE 1

Influence of the Oxidation of *n*-Butane, Butadiene, and Furan on the Physicochemical Characteristics of the $VOPO_4$ Catalysts, as Studied by XRD, ^{31}P MAS–NMR, and Laser Raman Spectroscopy

Catalyst	Reactant	XRD	^{31}P MAS–NMR[a]	Raman
α_{II} $VOPO_4$	(As prepared)	γ $VOPO_4$ (traces)	1	γ $VOPO_4$ (traces)
	Butane	—	0.91	—
	Butadiene	γ $VOPO_4$ (traces)	1.32	γ $VOPO_4$ (traces)
	Furan	—	1.22	—
β $VOPO_4$	(As prepared)	—	1	—
	Butane	—	3.2	—
	Butadiene	Pyro + carbon	3.7	Loss of definition
	Furan	Carbon	3.1	Carbon
γ $VOPO_4$	(As prepared)	α_{II} $VOPO_4$ (traces)		α_{II} $VOPO_4$ (traces)
	Butane	—	Crystallization increase	—
	Butadiene	α_{II} $VOPO_4$ (traces)		α_{II} $VOPO_4$ (traces)
	Furan	—		—
δ $VOPO_4$	(As prepared)	—	—	—
	Butane	α_{II} + δ $VOPO_4$	α_{II} + δ $VOPO_4$	α_{II} + δ $VOPO_4$
	Butadiene	α_{II} $VOPO_4$ + pyro	α_{II} $VOPO_4$	α_{II} $VOPO_4$
	Furan	α_{II} + δ $VOPO_4$	α_{II} + δ $VOPO_4$	α_{II} + δ $VOPO_4$

[a] Values correspond to ratio of the intensity of the rotating bands as compared to the central band.

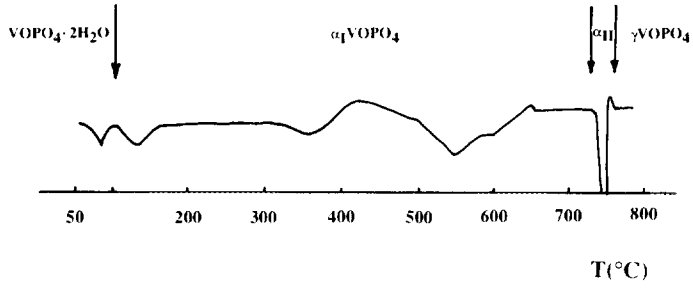

FIG. 1. DTA curve for oxidation under air of $VOPO_4 \cdot 2H_2O$ (arrows delimit the domains of stability of the different $VOPO_4$ phases).

MAS–NMR, laser Raman spectroscopy, and electron spin resonance. No changes in many characteristics of the α_{II} and γ $VOPO_4$ phases were observed after catalytic testing whatever the reactant molecules (butane, butadiene, and furan). Note that the α_{II} phase, as prepared, contained some γ phase as an impurity. This is due to the difficulty to obtain pure α_{II} $VOPO_4$ since the range of preparation temperature is very narrow, 730°C for α_{II} and more than 750°C for γ (Fig. 1). In the ^{31}P MAS–NMR spectrum, a slight increase of the intensity of the rotating bands with respect to the central peak was observed for α_{II} $VOPO_4$ after butadiene and furan oxidation (see Table 1). This intensity increase is indicative of an enhancement of the V^{4+} concentration in this phase, however, at a low level since no chemical shift was observed for the ^{31}P central peak.

For β $VOPO_4$, the intensity of the XRD peaks decreased by a factor of 2 upon butadiene oxidation reaction while broad new peaks appeared at ca 26.8 and 28.0° 2Θ (Fig. 2) which were attributed to some $(VO)_2P_2O_7$ and carbon amorphous entities generated during reaction. On the ^{31}P MAS–NMR spectra (Fig. 3), also a higher increase of the relative intensity of the rotation bands was observed as referred to the central peak (see Table 1), indicative of a higher reduction of this phase as compared to α_{II} $VOPO_4$ after butane, butadiene, and furan oxidation.

For δ $VOPO_4$, important transformations did occur upon catalytic reaction, particularly after butadiene and furan oxidation: the δ phase was changed into α_{II} phase. The XRD data (Fig. 4) were supported by the LRS and ^{31}P MAS–NMR results (Table 1). Note that after both butadiene and furan oxidation, the α_{II} (200) peak was enhanced, while the α_{II} (001) peak was decreased with respect to the pure α_{II} phase (3), indicating an epitaxial growth of the α_{II} phase on the δ matrix.

No detectable changes in the XRD, Raman, and ^{31}P MAS–NMR spectra were observed after catalytic oxidation of butane, butadiene, and furan on $(VO)_2P_2O_7$ and on the activated VPO catalyst. Only $(VO)_2P_2O_7$ was detected on both solids after reaction. As an example, XRD spectra are given for the activated VPO catalyst (Fig. 5).

Whatever the reactant molecule, the very high stability of $(VO)_2P_2O_7$ and the VPO catalyst is noteworthy. The latter fact is not surprising since it is known that the active VPO catalyst is composed mainly of $(VO)_2P_2O_7$. To the contrary, it is surprising that all the different $VOPO_4$ phases are either unmodified (α_{II} and γ), partly reduced and less crystalline (β), or result in another $VOPO_4$ phase (δ is partly transformed into α_{II}), but most of them, except δ $VOPO_4$, are unreduced even in the stationary state. As reduction was expected, we postulated that it should occur only on the surface and thus should be undetected by the previous techniques used.

The ESR technique, which is very sensitive to paramagnetic species, i.e., to V^{4+} cations, should then be of high interest for studying the samples before and after reaction. $(VO)_2P_2O_7$ and the activated VPO catalyst exhibited an intense almost symmetrical ESR line with no hyperfine (h.f.) splitting structure. An h.f. structure is only expected for diluted or dispersed V^{4+} or VO^{2+} cations ($I = 7/2$ gives rise to eight hyperfine lines) (Fig. 6). The peak-to-peak linewidths equal 0.9 and 1.3. 10^{-2} Tesla, respectively, with $g_{iso} = 1.961$ for both samples. The absence of hyperfine

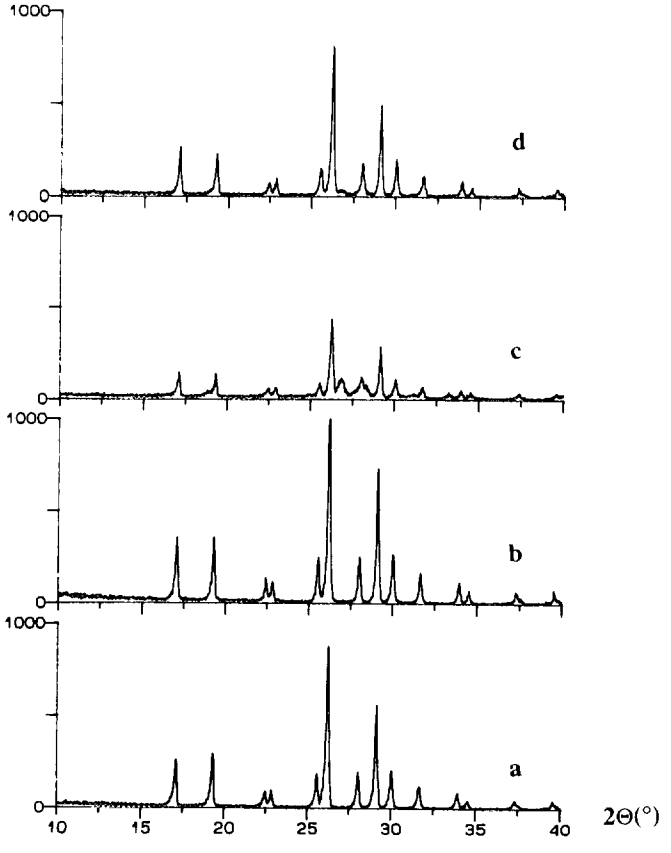

FIG. 2. XRD of the β $VOPO_4$ catalyst after butane (b), butadiene (c), and furan oxidation (d), referred to β $VOPO_4$ as prepared (a) (see Ref. (3)).

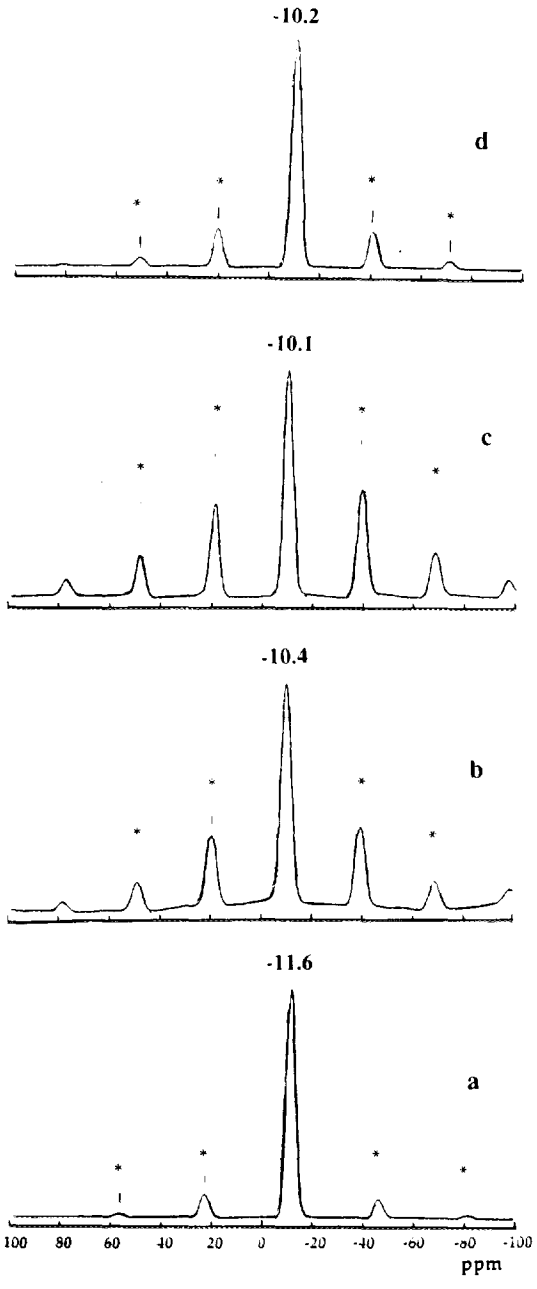

FIG. 3. Modification of the ^{31}P MAS–NMR spectra of β $VOPO_4$ as prepared (a) and after butane oxidation (b), butadiene oxidation (c), and furan oxidation (d). *indicates rotation bands.

structure is due to strong electron exchange interaction related to high V^{4+} cation concentration in the corresponding structures. A detailed analysis of the line shape shows that the spectrum for $(VO)_2P_2O_7$ (Fig. 6a) is in fact composed of two underlying lorentzian lines of width 0.8 and 1.8. $\times 10^{-2}$ Tesla respectively. The spectrum for the activated VPO catalyst (Fig. 6a) corresponds to a unique Lorentzian line. As the linewidth is related to the inverse of the spin lattice relaxation ($\Delta Hpp \propto (1/T1e) + (1/T2e)$), i.e., to the V^{4+} cation environment, the ESR results show that two types of VO^{2+} environment exist for $(VO)_2P_2O_7$ and a rather unique one for the activated VPO catalyst. From the examination of the two spectra it clearly appears that the magnetic properties of the two samples are different. This may be related to magnetically detected defects, as described in Ref. (10). No effect of butane or butadiene oxidation was observed in the ESR spectrum of $(VO)_2P_2O_7$. For the activated VPO catalyst, a very slight effect, if any, was observed after butane oxidation, while a broadening to 1.6–2.0 $\times 10^{-2}$ Tesla occured after butadiene oxidation. This indicates that the activated VPO catalyst is less stable than $(VO)_2P_2O_7$ and that its magnetic feature may be more easily modified when oxidoreducing catalytic conditions are changed (butadiene being a more reducing reactant than *n*-butane).

The case of the different $VOPO_4$ phases appears to be complex since the presence of V^{4+} cations was expected only after catalytic testing. In fact, relatively strong ESR spectrum was obtained for all phases, even before catalytic reaction. Such spectra are composed of a typical

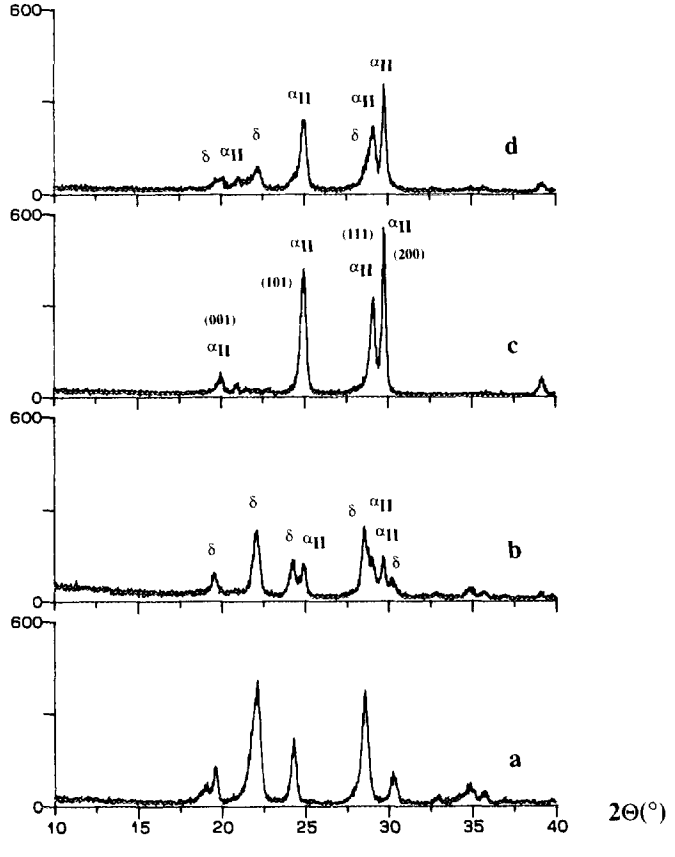

FIG. 4. XRD of the δ $VOPO_4$ catalyst after butane (b), butadiene (c), and furan oxidation (d), referred to δ $VOPO_4$ as prepared (a) (see Ref. (3)).

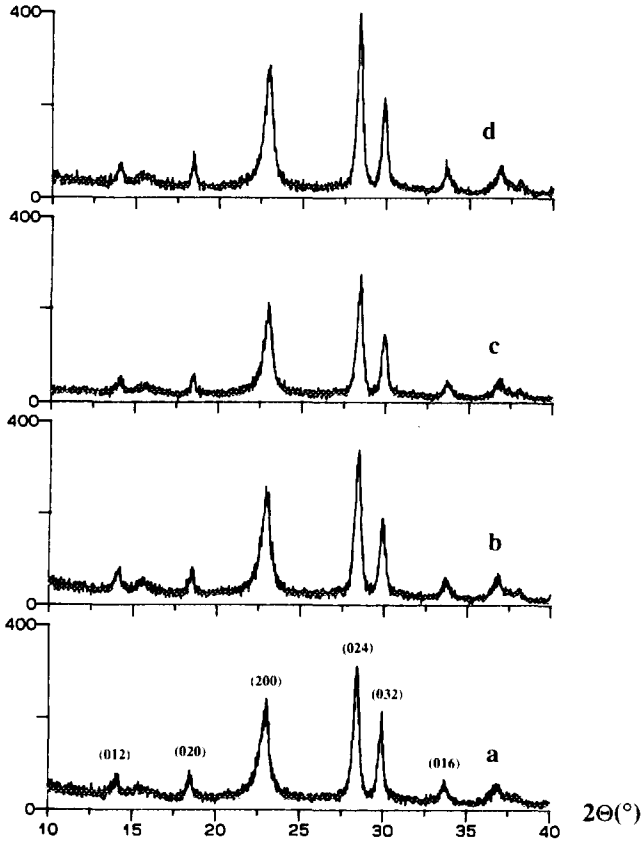

FIG. 5. XRD of the VPO catalyst after butane (b), butadiene (c), and furan oxidation (d), referred to the activated VPO catalyst as prepared (a) (see Ref. (3)). The indexation corresponds to the characteristic lines of $(VO)_2P_2O_7$.

VO^{2+} spectrum with hyperfine structure (powder spectra with eight components) (11) and a central line without hyperfine structure. The corresponding values were obtained:

α_{II}: $g_\perp = 1.970$, $g_\parallel = 1.925$ ($g_{av} = 1.955$);
β: $g_{iso} = 1.962$, $\Delta Hpp \sim 0.8 \times 10^{-2}$ Tesla;
γ: $g_\perp = 1.979$, $g_\parallel = 1.916$ ($g_{av} = 1.961$);
δ: $g_{iso} = 1.961$, $\Delta Hpp \sim 0.6 \times 10^{-2}$ Tesla.

Figure 7 shows the evolution of the EPR spectrum of δ $VOPO_4$ registered at −196°C after treatment under vacuum at room temperature and before (Fig. 7a) and after butane oxidation (Fig. 7b). It is noticeable that after butane oxidation, the spectrum exhibiting hyperfine structure has either disappeared or, at least, has strongly decreased while the other spectrum has an increased intensity without hyperfine structure. The first spectrum is attributed to dispersed VO^{2+} cation due to an incomplete oxidation of the precursor. Note that the ESR technique is particularly sensitive to trace impurities which can thus

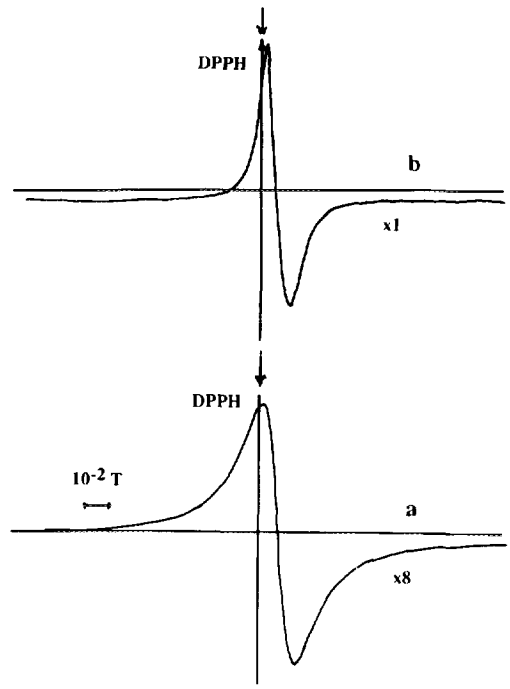

FIG. 6. ESR spectra recorded at −196°C of the activated VPO catalyst (a) and of $(VO)_2P_2O_7$ (b).

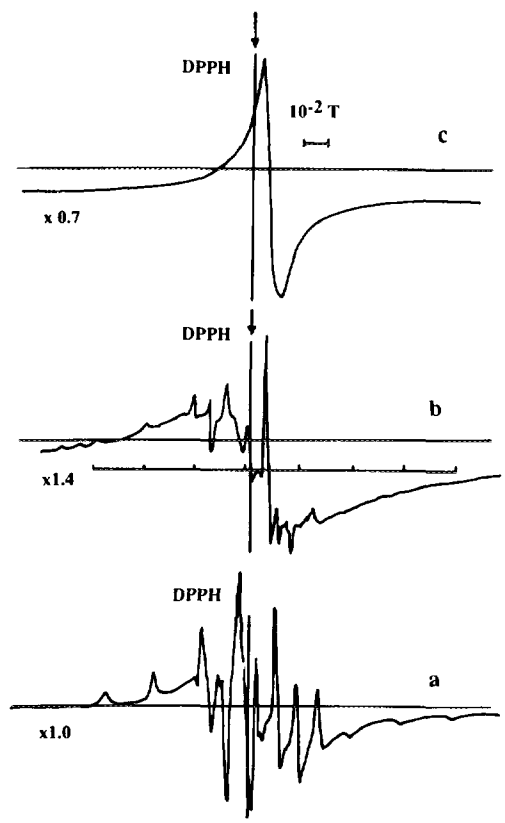

FIG. 7. ESR spectra recorded at −196°C of δ $VOPO_4$ as prepared (a) and after butane oxidation (b) and butadiene oxidation (c).

be detected. The second spectrum is attributed to a given V^{4+} phase (i.e., several V^{4+} cations at proximity as in $(VO)_2P_2O_7$. As its intensity increased with reaction, this indicates that upon butane oxidation conditions, some V^{4+} phase ensembles (or even as a phase) are formed even if they are not detected by the other techniques such as XRD and LRS.

These evolutions of the ESR spectra observed after butane oxidation were also observed after butadiene (Fig. 7c) and furan oxidation. They can be related to the evolution of the ^{31}P MAS–NMR spectra, since, as described above, the rotating band intensity, related to the presence of the V^{4+} domains, was observed to increase upon reaction.

DISCUSSION

A very deep evolution of the structure of δ $VOPO_4$ as evidenced by XRD, LRS, and ^{31}P MAS–NMR was observed after butane, butadiene, and furan oxidation reaction. This corresponds to a more or less important transformation into α_{II} $VOPO_4$. No such bulk evolution was observed for α_{II} and γ $VOPO_4$. The strong modification of δ $VOPO_4$ in comparison with the other $VOPO_4$ phases can be explained by the relatively low temperature of synthesis of this phase (450°C under oxygen) which approaches the temperature of butane, butadiene, and furan oxidation (1).

The case of β $VOPO_4$ seems to be different since crystallinity is decreased while partial reduction is observed, particularly under butadiene and furan oxidation (appearance of $(VO)_2P_2O_7$ by XRD). The use of EPR before and after butane oxidation shows that the situation is, however, more complicated. For all the $VOPO_4$ phases, butane oxidation develops V^{4+} ensembles and appears to favor the agglomeration of isolated V^{4+} ion still present after the preparation. This can also be detected by changes in the rotating band intensity by ^{31}P MAS–NMR. V^{4+} ensembles, with variable size, correspond to a local reduction of $VOPO_4$. These ensembles are sufficiently small so that they cannot be detected as $(VO)_2P_2O_7$ by XRD and LRS. The ESR technique also shows that the reduced V species are located at the surface of the samples, suggesting that only surface oxygen should be involved in oxidation of butane, in agreement with previous observations (12, 13).

We can now question which correlation can be established between the catalytic results for butane, butadiene, and furan oxidation (1) and the physicochemical informations which have been obtained on the reference VPO phases and the VPO catalyst after reaction. It is noticeable that the bulk evolution of the δ $VOPO_4$ phase into α_{II} does not appear to be followed by any peculiar catalytic behavior and especially the catalytic properties of α_{II} $VOPO_4$. However, as seen above, an epitaxial growth of α_{II} $VOPO_4$ on δ $VOPO_4$ was observed which should completely change its catalytic properties.

We previously proposed a model for the oxidation of butane to maleic anhydride on the VPO catalyst (14). This model was established from the consideration of the physicochemical evolution of a catalyst prepared by activation of the $VOHPO_4 \cdot 0.5H_2O$ precursor under an oxygen-free argon atmosphere of calcination to the butane/air atmosphere of catalysis. It was observed that best catalytic results corresponded to a limited number of V^{5+} sites forming small domains with a strong interaction with the $(VO)_2P_2O_7$ matrix and assumed to be preferentially located in the (100) crystal face. The formation of maleic anhydride may probably occur on the basal (100) $(VO)_2P_2O_7$ face with the participation of a suitable number of V^{5+} sites. In this previous study (14), we showed that side faces of $(VO)_2P_2O_7$ located in the [100] direction appeared to be faces for nucleation and growth of α_{II} and δ $VOPO_4$ and to be less selective as compared to the (100) face. During the activation of the VPO catalyst, the nucleated $VOPO_4$ phases observed in the first hours with $(VO)_2P_2O_7$ are redistributed as V^{5+} sites on/in the $(VO)_2P_2O_7$ matrix, thus giving a peculiar V^{4+}/V^{5+} distribution on the (100) face. This was evidenced from an *in situ* study using a Raman cell (15). On equilibrated VPO catalysts, and at stationary state, the oxidation of butane to maleic anhydride should thus depend on this superficial local V^{4+}/V^{5+} distribution in this (100) face. In Fig. 8, a scheme of reaction on the (100) $(VO)_2P_2O_7$ face for the oxidation of butane to maleic anhydride is shown. This scheme involves an alkoxide route with at least one bond between the catalyst and the reactant. The initial surface distribution of V^{4+} and V^{5+} sites indicated in Fig. 8 shows a local situation of the VPO catalyst at stationary state. All the electronic transfers between the *n*-butane molecule and the surface imply the existence of both V^{4+} and V^{5+} sites in a sufficiently close vicinity. Two possible models are postulated which imply a dynamic and static situation of the *n*-C_4 molecule:

(*i*) *The dynamic model.* In this first case, the *n*-butane molecule moves on the (100) $(VO)_2P_2O_7$ face until it is in contact with the favorable V^{4+}/V^{5+} steric situation which will initiate the first abstraction of hydrogen on C_2–C_3, as demonstrated by Pepera *et al.* (12),.

(*ii*) *The static model.* In this second case, the different steps of the *n*-butane transformation into maleic anhydride occur in the same area of the (100) $(VO)_2P_2O_7$ face. The local V^{4+}/V^{5+} distribution changes very rapidly by electron or O^{2-} transfers. Each step occurs when the favorable V^{4+}/V^{5+} distribution exists.

It clearly appears that the alkoxide route involves a

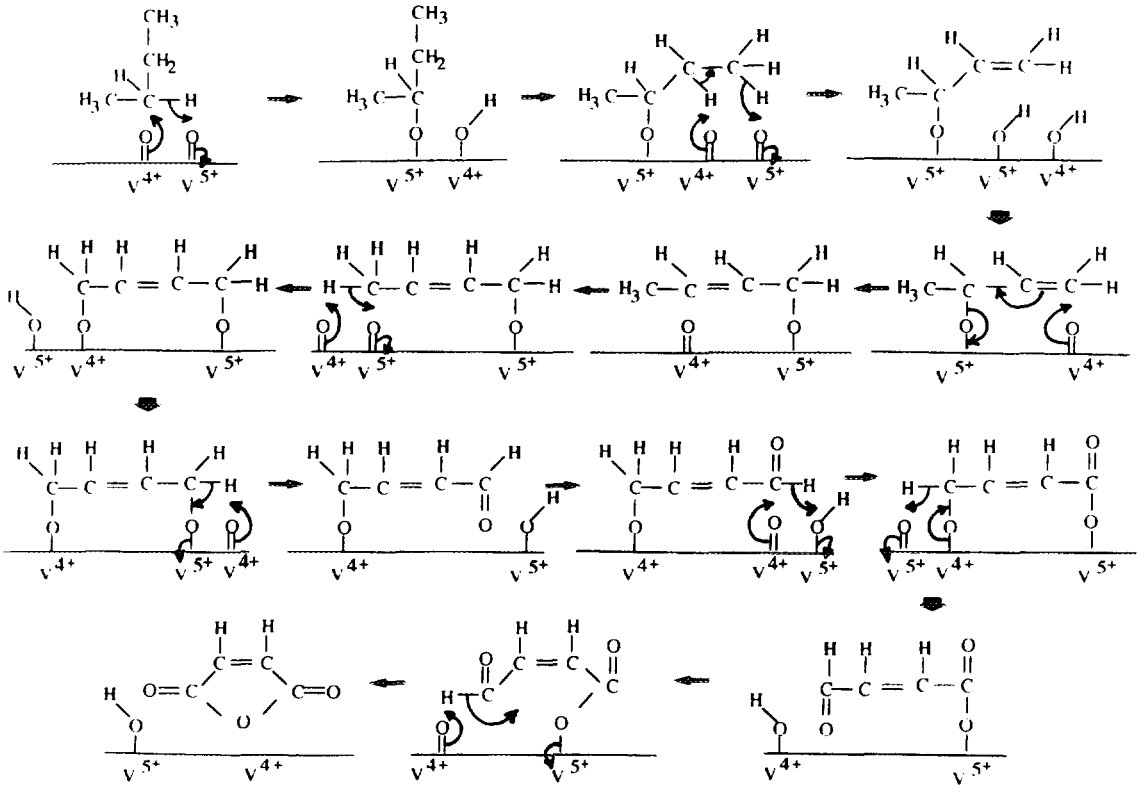

FIG. 8. Proposal for a reaction scheme for the oxidation of *n*-butane to maleic anhydride which implies the alkoxide route.

static model and a local site of a small size with a specific number of V atoms and a precise V^{4+}/V^{5+} distribution. The EPR study shows that under reaction on $VOPO_4$ phases, V^{4+} ensembles are created while isolated V^{4+} cations disappear, probably by oxidation. A different V^{4+}/V^{5+} distribution should thus be reached as compared to the (100) face of $(VO)_2P_2O_7$. The relatively comparable results observed in the reaction scheme (1) for the bu-

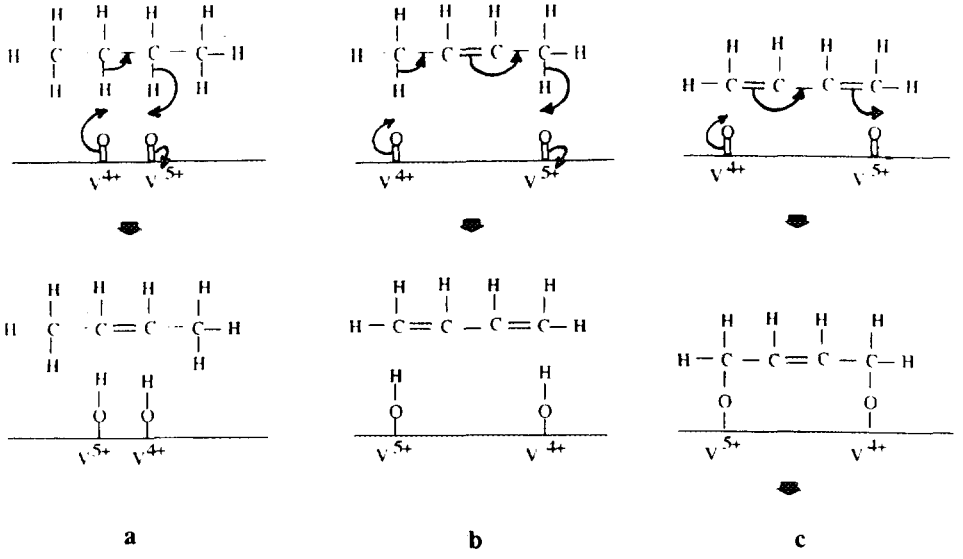

a b c

FIG. 9. Proposal for a reaction scheme for the oxidehydrogenation of *n*-butane to 2-butene (a) and 2-butene to butadiene (b), and the oxidation of butadiene to maleic anhydride (c). The final intermediate in (c) is presented in Fig. 8.

tane–maleic anhydride transformation for γ $VOPO_4$ (65.5; Fig. 12 in Ref. (1)) and δ $VOPO_4$ (60.7; Fig. 13 in Ref. (1)) as compared to $(VO)_2P_2O_7$ (62.6; Fig. 9 in Ref. (1)) indicate that a superficial V^{4+}/V^{5+} distribution should be reached similarly in butane oxidation conditions and different from those on α_{II} and β $VOPO_4$.

In Figs. 9 and 10, proposals are given for reaction schemes for the oxidehydrogenation of *n*-butane to 2-butene and oxidation of butadiene and furane to maleic anhydride. The mechanism of *n*-butane oxidation to maleic anhydride has been largely debated in the literature. The proposal given in Part I of this work (1) involves a direct route without desorption of the intermediates. In such a case, the active sites should be large enough to accommodate the butane molecule and to permit an eight hydrogen atom abstractions, three oxygen atom incorporations, and a 14-electron transfer. Taking into account the fact that good results for butane oxidation to maleic anhydride were obtained for γ and δ $VOPO_4$ as compared to $(VO)_2P_2O_7$ but not as good as for the activated VPO, we arrived at the conclusion that the surface of the catalysts should accommodate a specific number of V^{4+}/V^{5+} sites favorable to the butane oxidation to maleic anhydride and in a peculiar local distribution. This situation should be reached easily for the VPO catalyst, with more difficulty for $(VO)_2P_2O_7$, δ, and γ $VOPO_4$, and not reached for β $VOPO_4$ which is known to result majoritarly in total oxidation. Catalytic results should thus depend on a specific V^{4+}/V^{5+} sites isolation corresponding to an appropriate oxidoreduction situation, which, of course is depending on the materials but also on the catalytic conditions. Such a site isolation principle was first proposed by Grasselli (16). An active site model was described by Ziolkowski *et al.* on the (100) face of $(VO)_2P_2O_7$ (17). It implies the interaction of the *n*-butane molecule with five active oxygen bonded to vanadium cations and situated in a specific grouping of V atoms to accommodate the *n*-butane molecule. We can imagine in agreement with this model that the V^{5+} ensembles evidenced in our study by ^{31}P MAS–NMR on the VPO catalyst should correspond to these vanadium cations associated to these active oxygen atoms in the (100) face of $(VO)_2P_2O_7$ (14). If we assume that the oxidation state of vanadium should vary from +5 to +4 and vice versa during the catalytic reaction, several steps can be considered to explain the mechanism of butane oxidation to maleic anhydride in this face:

—The first two hydrogen atoms abstraction occuring on C_2–C_3 (12) and giving butene needs two electrons transfer and two vanadium atoms.

—The second two hydrogen atoms abstraction giving butadiene needs also two electrons to transfer and two vanadium atoms.

—The incorporation of the first oxygen atom to give the furan ring needs two electrons to transfer and also two vanadium atoms.

—Finally, the incorporation of the second and third oxygen atoms associated with the abstraction of four hydrogen atoms needs eight electrons and eight vanadium atoms.

It thus appears that the whole mechanism for butane oxidation into maleic anhydride should necessitate 14 vanadium atoms. However, it is obvious that some of these atoms should participate several times during these four steps so that the mechanism should need less than this number.

Such a proposal implies that the isolated V^{5+} active sites should exchange oxygen between the different steps in order to allow the V^{5+}/V^{4+} oxidoreduction cycle schematized below according to the suggestion by Bond for the VO_x/TiO_2 catalytic system for xylene oxidation to phtalic anhydride (18):

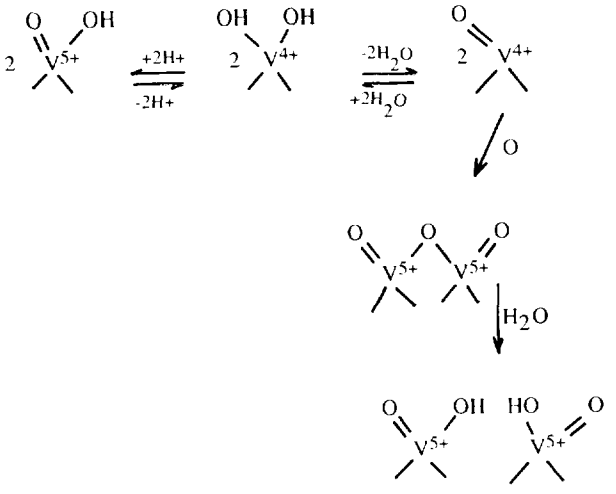

CONCLUSIONS

The present study shows that under butane oxidation conditions, $(VO)_2P_2O_7$ and the activated VPO catalyst do not change their structures as observed by XRD, Raman, and ^{31}P MAS–NMR. This is also the case for butadiene and furan oxidation. With the exception of δ $VOPO_4$, which is partly transformed into α_{II} $VOPO_4$, the $VOPO_4$ phases are not modified under the influence of the same reactants in catalytic conditions. From this study and Part I of this work (1), we can conclude that the mechanism for *n*-butane oxidation on VPO catalysts implies the participation of a limited number of superficial layers of the structure. There is no general consensus about the role of lattice and gas-phase oxygen in selective and complete oxidation reactions of C_4 hydrocarbons (19) and this as-

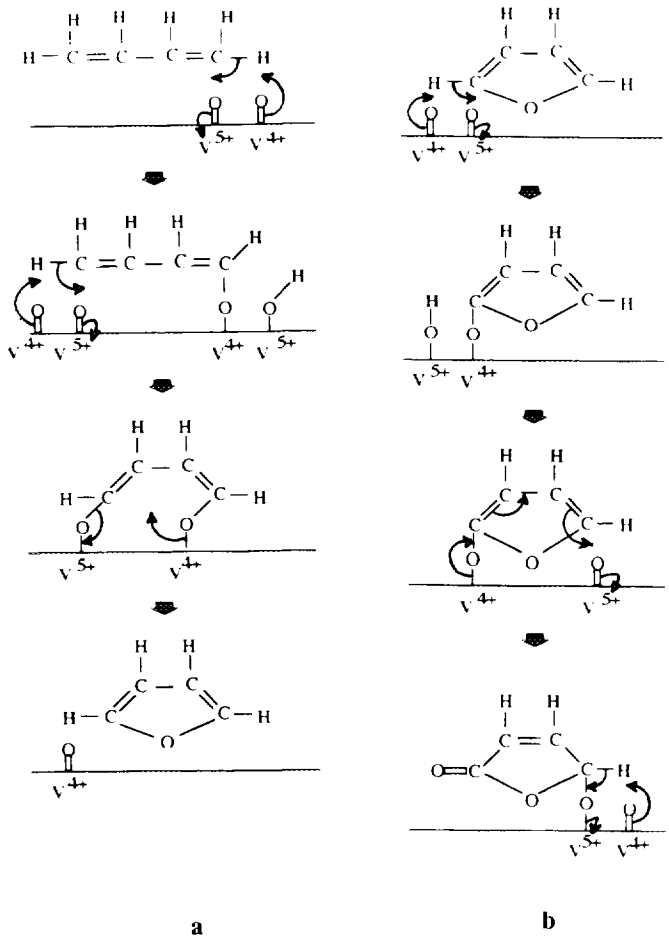

a b

FIG. 10. Proposal for a reaction scheme for the oxidation of butadiene to furan (a) and furan to maleic anhydride (b).

pect needs to be further studied (20). Our study shows that the situation of *n*-butane oxidation is highly different from that of the olefins oxidation for which the participation of the structure of the bulk is important (21, 22). We arrive at the conclusion that the catalytic results for butane oxidation to maleic anhydride should depend on the redox properties of V^{5+} ensembles on the $(VO)_2P_2O_7$ matrix. Their size, their number and their location should be very important to control the V^{4+}/V^{5+} redox which is responsible for the catalytic performances of the VPO catalyst. For the $VOPO_4$ phases, catalytic performances depend on their nature. The dehydrogenating character of α_{II} $VOPO_4$ should be associated with the difficulty to reduce its surface under catalytic conditions and thus to a very high superficial V^{5+}/V^{4+} density. For β $VOPO_4$, which is more easily transformed into $(VO)_2P_2O_7$ (1), the *n*-butane oxidation turns mainly to total oxidation due to a very high V^{4+}/V^{5+} superficial ratio, the opposite situation from α_{II} $VOPO_4$. The situation should be intermediate for γ and δ $VOPO_4$ which were also observed to be surprisingly active for *n*-butane oxidation: these two phases should present an intermediate reducibility as compared to α_{II} and β $VOPO_4$. For these two phases, it is suggested from the ESR study that ensembles of V^{4+} ions on the $VOPO_4$ (V^{5+}) matrix should play a comparable role to the VPO catalyst and finally reach a similar V^{4+}/V^{5+} superficial distribution suitable for the *n*-butane oxidation. The steric interaction *n*-butane/V^{4+}–V^{5+} sites on the surface of the pyrovanadate surface appears to be crucial at the different steps of the mechanism. This explains the specificity of the VPO catalyst for the oxidation of *n*-butane to maleic anhydride.

ACKNOWLEDGMENT

The authors thank Dr. Farid Ben Abdelouahab for the DTA experiment on the $VOPO_4 \cdot 2H_2O$ dihydrate.

REFERENCES

1. Zhang-Lin, Y., Forissier, M., Sneeden, R. P., Védrine, J. C., and Volta, J. C., *J. Catal.*, in press.
2. Centi, G., Trifiro, F., Ebner, J. R., and Franchetti, V. M., *Chem. Rev.* **88,** 55 (1988).
3. Ben Abdfelouahab, Olier, R., Guilhaume, N., Lefebvre, F., and Volta, J. C., *J. Catal.* **134,** 151 (1992).
4. Ladwig, G., *Z. Anorg. Allg. Chem.* **338,** 266 (1965).
5. Bordes, E., Courtine, P., and Pannetier, G., *Ann. Chim.* **8,** 105 (1973).
6. Bordes, E., and Courtine, P., *J. Catal.* **57,** 236 (1979).
7. Souchay, P., and Dubois, S., *Ann. Chim.* **3,** 88 (1948).
8. Johnson, J. W., Johnston, D. C., Jacobson, A. J., and Brody, J. F., *J. Am. Chem. Soc.* **106,** 8123 (1984).
9. Zhang-Lin, Y. J., Sneeden, R. P. A., and Volta, J. C., *Catal. Today,* **16,** 39 (1993).
10. Johnson, J. W., Johnston, D. C., and Jacobson, A. J., *in* "Preparation of Catalysts IV" (B. Delmon, Ed.), p. 181. Elsevier, Amsterdam, 1987.
11. Mériaudeau, P., and Védrine, J. C., *Nouv. J. Chim.* **2,** 33 (1978).
12. Pepera, M. A., Callahan, J. L., Desmond, M. J., Milberger, E. C., Blum, P. R., and Bremer, N. J., *J. Am. Chem. Soc.* **107,** 4883 (1985).
13. Okuhara, T., and Misono, M., *Catal. Today* **16,** 61, (1993).
14. Volta, J. C., Bere, K., Zhang-Lin, Y., and Olier, R., *in* "Catalytic Selective Oxidation" (S. T. Oyama and J. W. Hightower, Eds.), ACS Symposium Series 523, p. 217. American Chemical Society, Washington, DC, 1993.
15. Hutchings, G. J., Olier, R., and Volta, J. C., submitted for publication.
16. Grasselli, R., *in* "Surface Properties and Catalysis by Non Metals" (J. P. Bonnelle *et al.*, Eds.), p. 273. Reidel, Dordrecht, 1983.
17. Ziolkowski, J., Bordes, E., and Courtine, P., *J. Catal.* **122,** 126 (1990).
18. Bond, G. C., *J. Catal.* **116,** 531 (1989).
19. Centi, G., *Catal. Today* **16,** 5 (1993).
20. Centi, G., *Catal. Today* **16,** 147 (1993).
21. Grasselli, R. K., and Burrington, J. D., *Adv. Catal.* **30,** 133 (1981).
22. Keulks, G. W. and Matsuzaki, T., *in* "Adsorption and Catalysis on Oxide Surfaces" (M. Che and G. C. Bond, Eds.), p. 297. Elsevier, Amsterdam, 1985.